Journal of Medicinal Chemistry Article

J. Med. Chem. **2009,** *52,* 7157–7162 **7157**
DOI: 10.1021/jm901106t

The Role of Membranes in the Organization of HIV-1 Gag p6 and Vpr: p6 Shows High Affinity for Membrane Bilayers Which Substantially Increases the Interaction between p6 and Vpr.

Gilmar F. Salgado,*[,†] Alexander Vogel,[‡] Rodrigue Marquant,[§] Scott E. Feller,[⊥] Serge Bouaziz,[§] and Isabel D. Alves*[,∥]

[†]*Département de Chimie, Ecole Normale Supérieure, CNRS, UMR 8642, 24 rue Lhomond, 75231 Paris cedex 05, France,* [‡]*Institut für Biochemie und Biotechnologie, Martin Luther Universität Halle-Wittenberg, Kurt-Mothes-Str. 3, D-06120 Halle, Germany,* [§]*Unité de Pharmacologie Chimique et Génétique, Inserm U640, CNRS UMR8151, UFR des Sciences Pharmaceutiques et Biologiques, 4 avenue de l'Observatoire, 75270 Paris Cedex 06, France,* [⊥]*Department of Chemistry, Wabash College, 301 W. Wabash Avenue, Crawfordsville, Indiana 47933, and* [∥]*UMR 7203, Laboratoire des Biomolecules, FR 2769, and CNRS, F-75005, Paris, France*

Received August 24, 2009

The molecular mechanism by which HIV-1 Gag proteins are targeted and transported to the plasma membrane after ribosomal synthesis is unknown. In this work, we investigated the potential interaction of p6 and Vpr with model membranes and have determined their binding constants. Plasmon waveguide resonance (PWR) experiments showed that p6 strongly interacts with membranes (K_d ~40 nM), which may help explaining in part why Gag is targeted to and assembles into membranes by coating itself with lipids. Moreover, a substantial increased affinity of Vpr for p6 was observed while in a membrane environment. In order to further investigate the molecular properties behind the high affinity to model membranes, molecular dynamics simulations were carried out for p6 with a dodecylphosphocholine (DPC) micelle. The results indicate an integration route model for Vpr into virions and may help explain why previous reports failed to detect p6 in virion core preparations.

Introduction

During human immunodeficiency virus type-1 (HIV-1)[a] infection, cleavage of Gag polypeptide is necessary in the early replication phase.[1,2] Gag p6 is one of the cleavage products and promotes virion release by budding from the host-cell plasma membrane. Without p6, HIV-1 virus particles would accumulate in the bilayer rendering the full infection cycle incomplete.[3,4] Moreover, recent studies strongly support the idea that the sorting mechanism may involve interactions with cellular partners, such as TSG101 and Alix, and specific short sequence regions (late domains) in p6 (e. g., P(T/S)AP10 or YPL38).[5−9,16] These regions would interact directly with a component of the endosomal sorting complex (TSG101) or indirectly via Alix.[10] Even though much remains to be clarified, a growing number of models converged by placing p6 in a central role during the virus-budding process.[11,14,16,19] Each HIV-1 virion may contain ~5000 copies of Gag,[11] which is perceived to be disposed in a radial manner around the inner leaflet of the lipid bilayer, specifically attached by the N-terminal portion of Gag through the myristylated part of Matrix (MA).[11,12,13,14,19] During the final process of infection, Gag proteins alone appear sufficient to promote the assembly and release of immature virus-like particles.[12,15] Gag p6 has also been shown to be extensively implicated in Vpr association and uptake into the virions during their release from infected cells.[12,17,36]

Here we present for the first time, dissociation constants concerning the interaction of Gag p6 ($p6_{1-52}$) and Vpr with membrane models. Differential scanning calorimetry (DSC) was used to probe the effect of p6 and Vpr in the phase transition of DMPC multilamellar vesicles (MLVs). The affinity of p6 to a solid supported egg PC bilayer was monitored by plasmon waveguide resonance (PWR). We also tested whether Vpr interaction with the bilayer would be affected by the presence of p6 by measuring the dissociation constants; PWR spectroscopy principles are thoroughly described elsewhere,[23−27] and it has been very successful in examining the interaction of peptides and proteins with membranes.[22−25] Additionally, we performed molecular dynamics simulation of p6 in a DPC micelle to provide a better description of the molecular properties underneath the interaction with membrane models.

Results

Probing the effects of p6, p6ct and Vpr on DMPC Lipid Phase Transition by DSC. The interaction of p6, p6ct, and Vpr with lipids was monitored by following the perturbation of the peptides on the lipid phase pretransition arising from the conversion of L_{β}' to P_{β}' (T_{pre}) and also the main phase transition corresponding to the conversion from P_{β}' to L_{α} (T_m) upon peptide/lipid interaction. The interaction of p6, p6ct, and Vpr with DMPC MLVs clearly affects the thermotropic lipid behavior with complete abolishment of the

*To whom correspondence should be addressed. E-mail addresses: gilmar.salgado@ens.fr; isabel.alves@upmc.fr. Mailing address (I.D.A.): UPMC, UMR 7203, case courier 182, 4 place Jussieu, 75005 Paris, France. Phone (G.F.S.): +33 1 44323344, Fax (G.F.S.): +33 1 44323397. Phone (I.D.A.) +33 1 44275509, Fax (I.D.A.): +33 1 44277150.

[a] Abbreviations: CHARMM, Chemistry at Harvard Macromolecular Mechanics; DSC, differential scanning calorimetry; DMPC, dimyristoylphosphatidylcholine; DPC dodecylphosphocholine; egg PC, egg phosphatidylcholine; GAG, group-specific antigen; HIV-1, human immunodeficiency virus type 1; HOBt/DCC, hydroxybenzotriazole/*N*,*N*′-dicyclohexylcarbodiimide; HPLC, high-performance liquid chromatography; MD, molecular dynamics; MLV, multilamellar vesicles; PWR, plasmon waveguide resonance; TFA, trifluoroacetic acid.

Published on Web 11/02/2009

pretransition, which arises from the tilting of the hydrocarbon chains. Moreover, the perturbation is also demonstrated by reduction of the main phase transition temperature (T_m), the cooperativity, and the enthalpy (Table 1 for thermodynamic parameters and Figure S1, Supporting Information). The enthalpy of the main phase transition is mainly due to the disruption of van der Waals interactions between the fatty acid chains, and perturbations on this transition are indicative of some intercalation of the peptide between the fatty acid chains, thus explaining the decrease in the cooperativity of the lipid phase transition (Table 1). The reduction in the T_m by the peptides indicates their favorable interaction with the fluid *vs* gel phase. These results support a model where the peptide is adsorbed within the lipid head groups with some perturbation of the fatty acid chains caused by the direct interaction of hydrophobic side chains residues, which insert into the bilayer fatty acid chain region.

The Interaction of p6 with Egg PC and of Vpr with Egg PC Bilayer Containing p6. The affinity of Vpr to p6 was monitored by following the PWR spectral changes upon incremental additions of Vpr to the cell sample containing an egg PC lipid bilayer in which p6 has been incorporated. The addition of p6 induced significant PWR spectral changes both for *p*- and *s*-polarized light indicating that the peptide is binding to and inducing lipid reorganization in the bilayer. A binding constant of 34 nM was obtained for the interaction of p6 with an egg PC bilayer (Table 2). Graphical analysis of the PWR spectral shifts[26] indicates that the peptide induced spectral changes and those are mainly caused by alterations in mass (Table 3). The addition of Vpr to the egg PC bilayer containing p6 led to PWR spectral changes that result both from the interaction of Vpr with p6 and from that of Vpr with the egg PC bilayer. Taking that into account, the affinity of Vpr to an egg PC bilayer (in the absence and presence of p6) was determined (Figure 1 and Table 2). A considerably higher affinity was observed for the interaction of Vpr with an egg PC bilayer in presence of p6 ($K_d = 0.1\ \mu M$) than in the absence of p6 ($K_d = 70\ \mu M$). The data confirm that there is a considerably stronger interaction between Vpr and p6 within a membrane environment (Table 2).

The Interaction of p6ct with Egg PC and of Vpr with Egg PC Bilayer Containing p6ct. Using PWR, an affinity of 56 nM was observed for the interaction of p6ct with an egg PC bilayer (Table 2, results obtained from ref 20). This value is quite comparable to that obtained for p6 (34 nM), suggesting a minor role of the N-terminal side of p6 on bilayer interaction (Tables 2 and Figure 3). Additionally, the spectral changes are more anisotropic for p6ct (larger difference between the spectral shifts observed with *p*- and *s*-polarization) when compared with p6, which translates into differences in terms of mass and structural changes. Concerning the interaction of Vpr with the egg PC bilayer containing p6ct, the results point to similar spectral changes to those observed with p6 (Figure 2, Table 3). A lower affinity is observed for the interaction of Vpr with the p6ct-containing bilayer than with the p6-containing one (Table 2). A summary of the affinity of the different peptides and a membrane can be appreciated in Figure 3A.

Molecular Dynamics: The Interaction of p6 with DPC Micelle. During the 63 ns period of the MD simulation, p6 was always at the surface of the DPC micelle, and some important changes in its structure started to occur after 10−15 ns. Some of the most relevant features correspond to changes in the α-helix length and the insertion of residues inside the hydrophobic core of the micelle. As expected the α-helices 1 and 2 (HI and HII) become better defined over the course of the simulation. Reported lengths were 7.6 and 15.7 Å for HI (F17−T21) and HII (L38−S47), respectively, for the starting p6 sequence (PDB code 2c55),[30] while we observe 8.6 and 24.2 Å for HI (E13−F17) and H2 (I31−F46), respectively (average for the last nanosecond, Figure 4), in the 63 ns MD run. A similar dependence on the environment has been observed for buforin II.[41] Notably, HI shifted toward phenylalanine residues 15 and 17 slightly modifying the initial structure, emphasizing the importance that the solvent may have when determining protein structures and protein−protein interactions (the 2c55 structure was determined in 50% aqueous TFE mixture). During the 63 ns MD run, Phe45 shows a behavior somehow different from the other two phenylalanine residues. Residue Phe45 seems to adopt a position where the side chain main axis (Cα−Cz)

Table 1. Thermodynamic Parameters Obtained by DSC for the Interaction of p6, p6ct, and Vpr with DMPC MLVs[a]

peptide	T_{pre}	ΔH_{pre} (kcal/mol)	T_m	ΔH_m (kcal/mol)	$\Delta T_{1/2}$
DMPC alone[b]	8.3	0.8	22.8	6.6	0.7
DMPC + p6ct[b]	*c*	*c*	20.9	4.5	2.3
DMPC + p6	*c*	*c*	20.9	4.8	2.6
DMPC + Vpr	*c*	*c*	21.2	5.8	2.6

[a] The experiments were performed at a peptide/lipid ratio of 1/100. [b] Values extracted from ref 20. [c] Transition completely abolished.

Table 2. Binding Affinities for the Interaction of p6 and p6ct with the Lipid Bilayer and for the Interaction of Vpr with the Lipid Bilayer in Absence and in Presence of p6 and p6ct as Determined by PWR

peptide (in solution)	bilayer + bound peptide	K_d (μM)
p6	egg PC	0.034
p6ct[b]	egg PC	0.056
Vpr[b]	egg PC	70
Vpr	egg PC + p6	0.1
Vpr[b]	egg PC + p6ct	0.8

[a] K_d values were obtained with s-polarization data by plotting the resonance minimum angle for the incremental peptide addition and fitting this using an hyperbolic binding curve (see Experimental Section for details). [b] Values extracted from ref 20.

Table 3. Resonance Positions Shifts Observed upon Peptide Binding to an Egg PC Bilayer in Absence or Presence of Bound Peptide and Corresponding Mass and Structural Changes as Obtained from Graphical Analysis of the PWR Spectra[a]

		spectral shifts (mdeg)		graphical analysis	
peptide	bilayer + bound peptide	p-pol	s-pol	mass changes (%)	structural changes (%)
p6	egg PC	−20	−26	80	20
p6ct	egg PC	−4	−18	60	40
Vpr	egg PC	−13	−19	77	23
Vpr	egg PC + p6	−24	−38	76	24
Vpr	egg PC + p6ct	−23	−35	76	24

[a] Spectral shifts are those obtained for the saturated system (maximal peptide addition for which no spectral shifts were observed). Graphical analysis performed as in ref 26 provides an estimative of how much of the spectral changes are due to mass changes and to structural changes.

seems on average perpendicular to the micelle surface protruding inside the micelle hydrophobic core as an anchor point, while Phe15 and Phe17 side chains seem to adopt a "paddling" movement parallel to the micelle surface. This effect may be driven by the fact that both Phe15 and Phe17 are in opposite sides of the small helix HI and that the perpendicular insertion of one side chain would make the other turn and expose further to the water thereby stabilizing the helix orientation. Curiously, Phe15 and Phe17 are placed at the center of HI separated by Arg16, and both phenylalanine residues are flanked by the hydrophilic and negatively charged residues Glu12 and Glu13 on one side and Glu19 and Glu20 on the other. This structural disposition seems pertinent and can potentially aid in sustaining the two hydrophobic phenylalanine side chains "floating" at the micelle surface (Figure 4). On average, the greatest distance from Phe15 to Phe17 is ~13.5 ± 1.2 Å (Cz−Cz), creating a large exposed hydrophobic surface, which may act as a docking site for other partially hydrophobic proteins that are not very soluble as in the case of Vpr. Otherwise, there are no other major stretches of hydrophobic residues that keep the peptide adsorbed to the micelle surface, except for sequences of one or two dispersed residues as the case of six proline residues spread over the remaining sequence, an effect not seen in Pro49, which is totally exposed to the solvent, a consequence of the hydrogen bonding between Asp48 and Arg42. It is worth mentioning that the first eight residues of the N-terminus of p6 seem to establish around 50% of all hydrogen bonds found with the phosphate groups of DPC, from a total of 10−12 hydrogen bonds found in each structure in the last 10 ns. As expected, DPC headgroups do not interact extensively with the protein hydrophobic residues, and only polar side chain residues seem to satisfy the hydrogen-bonding interactions. Thus our results suggest a strong interaction with the DPC micelle head groups besides the hydrophobic interaction.

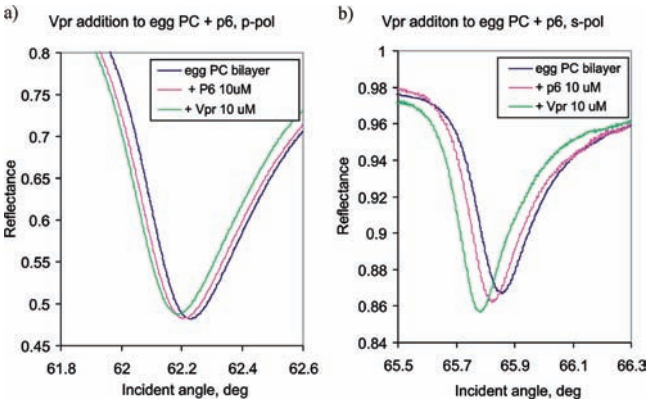

Figure 1. PWR spectra series depicting the interaction of Vpr with an egg PC planar membrane containing p6, using (a) *p*- and (b) *s*-polarized light excitation. All spectra were measured at 25 °C with 632.8 nm exciting light.

Discussion

In this study, we have determined the dissociation constants and thermodynamic parameters for the interaction of p6 with lipid bilayer membrane models, and we extended the discussion to include previous results obtained with p6ct.[20] We also probed the interaction of Vpr with a membrane model in the absence and in the presence of p6. Moreover, molecular dynamics simulation was performed in a system composed of p6 and a DPC micelle, providing complementary information concerning the molecular properties behind the adsorption of p6 to the membrane. Concerning the PWR studies, in all peptide to lipid interactions reported above, negative spectral shifts for both polarizations were observed (Table 3).

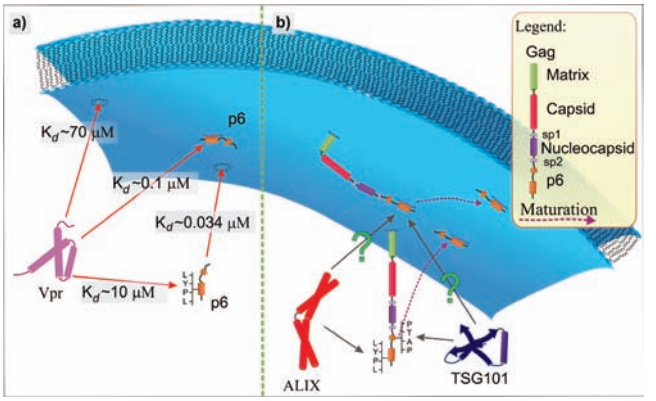

Figure 3. Summary of the binding constants for p6 and Vpr obtained for a bilayer of egg PC (a). Each arrow represents a binding event with its K_d on top of the respective red arrow. (b) Alix and Tsg101 may compete for the same binding regions in p6 as Vpr. The fact that Gag exists in excess with respect to Vpr may diminish the competition effect. It is still unclear whether both Alix and Tsg101 can bind to p6 incorporated in membranes and whether multiple binding is possible.

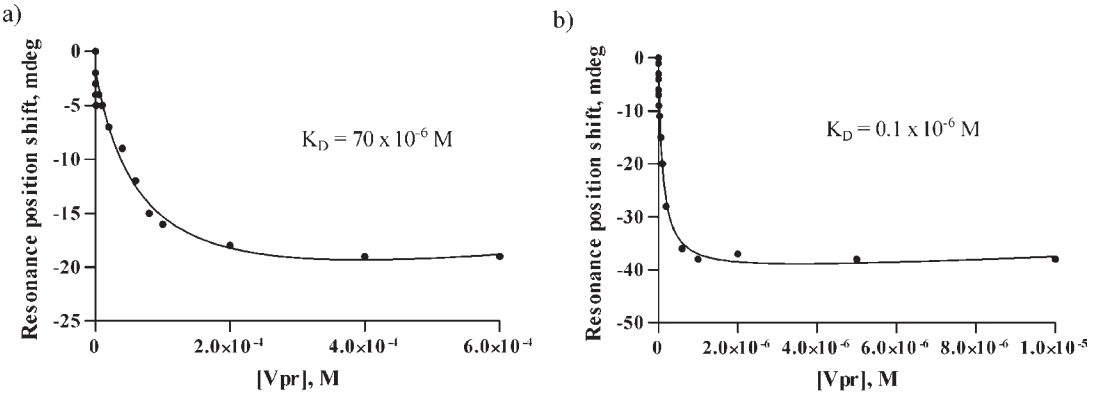

Figure 2. Interaction between Vpr and an egg PC planar lipid bilayer in the absence (a) and in the presence (b) of incorporated p6 measured by PWR. Dissociation constants are obtained by plotting the PWR spectral shifts obtained with the *s*-polarized light upon incremental additions of Vpr and fitting through a hyperbolic binding.

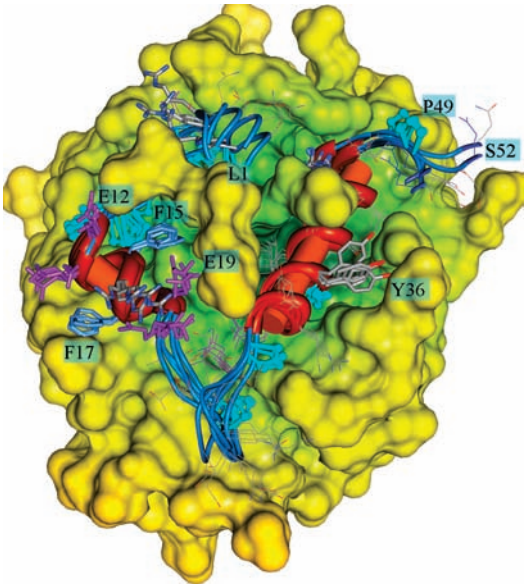

Figure 4. Schematic representation of five p6 structures adsorbed to a DPC micelle (yellow), as extracted from the final nanosecond of a 63 ns MD run with a time step of 2 fs. Molar ratio 1:100 (peptide/DPC). Proline, phenylalanine, and aspartate are colored cyan, blue, and pink, respectively.

When represented on a (s, p) coordinate system for mass and structural anisotropy changes,[26] all peptide-induced changes fall into the third quadrant of the plot (negative values for both *p*- and *s*-shifts) meaning that the mass changes they induce correspond to decreases in the mass density of the lipid bilayer. A decrease in mass density of the system, where mass is being added (peptide addition), can only be explained by lipid removal accompanied by structural rearrangements. Such effect could be explained by an efflux of lipid toward the Plateau−Gibbs border to accommodate peptide insertion between the lipid molecules. Such a process is accompanied by structural rearrangements of the proteolipid film that account for around 20% structural change (80% for mass change) for Vpr and p6 interaction with bilayer and 40% for p6ct. This is well supported by the considerable effects of p6, p6ct, and Vpr in the DMPC lipid phase transition observed with DSC (Table 1, Figure S1, Supporting Information). The highly anisotropic change observed upon p6 and p6ct addition to egg PC bilayer would indicate that this peptide, which intrinsically possesses an anisotropic structure (α-helix),[20,30] places itself with the long axis parallel to the lipid bilayer surface. The larger spectral changes observed for Vpr interaction with a bilayer containing p6 and p6ct relative to a bilayer alone may be related to structural changes that both p6 and Vpr undergo when these two peptides interact together. Bridging all the results leads us to conclude that both peptides, p6 or p6ct and Vpr, adsorb to the surface of membrane models with high affinity and that Vpr interaction is highly enhanced by the presence of p6. Moreover, as emphasized by MD simulations, the degree of membrane penetration seems to be confined to the first leaflet, not transposing or inserting across the bilayer.

Now the question that one may pose is when does this interaction with membranes start? Is the polypeptide Gag directly adsorbed to endoplasmic reticulum (ER)/Golgi membranes immediately after the translational process?

Previous studies have shown that deletions within the MA domain did not prevent viral assembly but rather redirected assembly and budding of virus particles to the membranes of the ER, and some particles, although defective in glycoproteins, were able to bud at the plasma membrane.[33] Although many results suggest that Gag can interact with membranes, it is difficult to precisely determine which part of Gag contributes to that phenomenon and to what extent. Apparently, being able to interact with membranes immediately after translation may be a fast way of compartmentalizing, regrouping, and also targeting the virion constituents very efficiently to the membrane for budding.[37,40] In this process, p6 seems to have the capacity to play an important role. Our results correlate well with previously reported studies,[18,21] showing that HIV-1 Gag proteins can partition directly to membranes without the aid of other cellular factors and also that membranes might serve as a nonspecific binding partner for virion particle assembly initiation.[22,37] With an approximate ratio of Gag/Vpr of 7:1,[11] p6 seems to be present in sufficiently large quantities to interact with other partners besides Vpr (e.g., Alix and Tsg101). This is a major step in HIV-1 life cycle, where p6 helps not only to target Gag to the cellular membrane[5,9,10] but most importantly to direct recently formed virions toward a clear pathway to escape from the cell interior by interacting with Alix and Tsg101. In this study, we also clearly demonstrate the preference of Vpr to interact with p6 adsorbed into membranes ($K_d \approx 0.1$ μM) rather than the membrane-free form of p6 ($K_d \approx 10$ μM, unpublished results), Figure 3. Previously we have identified the primary binding region in p6ct, which interacts with Vpr as being the ELYP37 sequence.[20] The MD data presented here expanded to the full p6 domain shows that when only the p6 sequence 32−52 is analyzed in the micelle surface, it does orient similarly as p6ct, exposing Tyr36 to the solvent in the same manner and inserting Phe45 into the micelle core as well (Figure 4). Nevertheless we cannot exclude other binding regions more toward the N-terminus, supported by the results of Table 2, which shows that the binding affinity is higher for p6 compared with p6ct, 0.1 vs 0.8 μM respectively. One important aspect that needs to be clarified is whether this property still holds for Alix and Tsg101, as well as whether multiple binding is possible in presence of membranes. Our results are compatible with interaction between Alix and p6, based in the integrity of the LYPXnL motif near the C-terminus of Gag,[35] based on the fact that Tyr36 seems well exposed to the solvent (Figure 4). In summary, the very strong affinity of p6 for membranes and the lower but still significant affinity for Vpr may help explain why in previous studies[38,39] the authors unexpectedly failed to detect the presence of p6 in virion core preparations, despite the presence of Vpr in the same cores. It seems, as pointed out in those studies that the mechanism of Vpr incorporation into the assembling particles diverges from that which directs Vpr toward the virion core.

Here we demonstrate clear evidence for specific interaction of p6 not only with membranes but also with Vpr, which will further improve our perception of how important this peptide is for the HIV-1 budding mechanism. We also hope that our results will contribute to the broad discussion concerning the viral particle organization, since many simplistic and rigid models describe Gag as a rod-like molecule arranged perpendicular to the membrane surface, with the N-terminal matrix domain of Gag directly interacting with the membrane. This simplistic view, more specifically concerning p6 organization, is not compatible with numerous experiments[18,20,21,38,39] including ours. Finally, we believe that these results will enrich the understanding concerning one of the biggest mysteries of Gag proteins, aimed at dissecting the determinants of the

membrane targeting and binding during budding immediately after ribosomal synthesis.

Experimental Section

Peptide Synthesis. Vpr and p6ct synthesis is described elsewhere,[20] Gag p6 (1-LQSRPEPTAP PEESFRSGVE TTTPPQKQ-EP IDKELYPLTS LRSLFGNDPS SQ-52) was synthesized similarly by a solid-phase Fmoc strategy. The method employs a small-scale Fmoc strategy on an Applied Biosystem synthesizer model ABI431A with Wang LL resin (0.48 mmol/g), and amino acids were purchased from Novabiochem. The p6 final extract crude amount was estimated to be ~480 mg. The resulting mixture was purified by reverse-phase HPLC (C4 column 300 Å, 5 μm, 250 mm × 10 mm, Ace) using H_2O/0.05% TFA mixture and acetonitrile as the mobile phase. A 20−35% linear gradient of acetonitrile was used over a 120 min run for optimal purification. The peptide was purified by HPLC as described before[20] and analyzed by mass spectroscopy showing a parent peak m/z 5806.9 (error of $<0.002\%$ from attending mass), with a final purity of ~98%.

Differential Scanning Calorimetry. Multilamellar vesicles (MLVs) composed of 1 mg/mL of DMPC (Avanti Lipids) in 10 mM sodium acetate, 30 mM NaCl, pH 3.5, were used for DSC studies. The calorimetry was performed on a high-sensitivity differential scanning calorimeter (Calorimetry Sciences Corporation). A scan rate of 1 °C/min was used with a delay of 10 min between sequential scans (five heating and cooling scans were performed) in a series that allows for thermal equilibration. Peptide/lipid molar ratios of 1/100 were used in those studies, and the peptide was added to MLVs after their formation. Data analysis was performed with the fitting program CpCalc (CSC) and plotted with Igor (WaveMetrics).

Plasmon Waveguide Resonance. The method to prepare the self-assembled single solid-supported planar lipid bilayer composed of egg PC (Avanti Lipids) has been described elsewhere.[23−25] The same buffer employed for DSC was used here, and the experiments were performed at 25 °C. After bilayer equilibration, the peptide (p6, p6ct, or Vpr) is injected into the cell, and spectra are followed until equilibrium is reached, after which a second injection is added, and so on, in an incremental fashion. For the studies of Vpr interaction with p6 and p6ct, the spectra become stabilized when concentrations of p6 or p6ct in the PWR cell sample reach ~10 μM, after which the cell was flushed with buffer to remove any partially unbound peptide. Following that, Vpr interaction with the egg PC bilayer containing p6 or p6ct was monitored in the same fashion. The dissociation constant was obtained for the interaction of Vpr with the egg PC bilayer, with or without p6ct or p6. The resonance minimum position was measured as a function of the ligand concentration and fit using a hyperbolic binding curve (GraphPad).

Molecular Dynamics. The program CHARMM[28] was used for system construction, simulation, and analysis, employing the CHARMM lipid force field including recent refinements for saturated chains.[29] The p6 structure was taken from the PDB database (PDB code 2c55)[30] and reconstituted into a former 60 ns simulation where the C-terminus (residues 32−52) of p6 was simulated in a DPC micelle.[20] The full-length p6 was aligned such that residues 32−44, which are part of a stable α-helix, overlapped with the C-terminal p6 peptide from the former simulation. The system consisted of 1 peptide, 100 DPC molecules, and 6165 water molecules. To account for the experimental salt concentration and to make the system neutral overall 2 sodium and 5 chloride ions were added to the simulation. All simulations were carried out with constant normal pressure (1 atm) and constant temperature (20 °C), using extended system algorithms.[31] Electrostatic forces were computed with the smooth particle mesh where bonds involving hydrogen atoms were constrained by means of the SHAKE algorithm.[32] The simulation was carried out for ~63 ns using a 2 fs time step. Figure 4 was prepared with UCSF Chimera.[34]

Acknowledgment. This work was supported by the French Agency for AIDS Research (ANRS), by Sidaction (Ensemble contre le SIDA), and by the "Exzellenznetzwerk Biowissenschaften" funded by the federal state of Sachsen-Anhalt (Germany). A.V. was the recipient of a postdoctoral scholarship from the Deutsche Forschungsgemeinschaft (VO1523/1-1). G.F.S. was supported by a postdoctoral fellowship from the Centre National de la Recherche Scientifique (CNRS). S.E.F. thanks the NSF and NIH for support through Grants MCB-0543124 and PHS 2 PN2 EY016570B, respectively.

Supporting Information Available: The thermogram obtained using differential scanning calorimetry and the evolution of the rmsd for the MD simulation. This material is available free of charge via the Internet at http://pubs.acs.org.

References

(1) Kawamura, M.; Shimano, R.; Inubushi, R.; Amano, K.; Ogasawara, T.; Akari, H.; Adachi, A. Cleavage of Gag precursor is required for early replication phase of HIV-1. *FEBS Lett.* **1997**, *29*, 227–230.
(2) Wiegers, K.; Rutter, G.; Kottler, H.; Tessmer, U.; Hohenberg, H.; Krausslich, H. G. Sequential steps in human immunodeficiency virus particle maturation revealed by alterations of individual Gag polyprotein cleavage sites. *J. Virol.* **1998**, *72*, 2846–2854.
(3) Gottlinger, H. G.; Dorfman, T.; Sodroski, J. G.; Haseltine, W. A. Effect of mutations affecting the p6 gag protein on human immunodeficiency virus particle release. *Proc. Natl. Acad. Sci. U.S.A.* **1991**, *88*, 3195–3199.
(4) Demirov, D. G.; Orenstein, J. M.; Freed, E. O. The late domain of human immunodeficiency virus type 1 p6 promotes virus release in a cell type-dependent manner. *J. Virol.* **2002**, *76*, 105–117.
(5) Fujii, K.; Hurley, J. H.; Freed, E. O. Beyond Tsg101: The role of Alix in 'ESCRTing' HIV-1. *Nat. Rev. Microbiol.* **2007**, *5*, 912–916.
(6) Freed, E. O. The HIV−TSG101 interface: Recent advances in a budding field. *Trends Microbiol.* **2003**, *11*, 56–59.
(7) Garrus, J. E.; von Schwedler, U. K.; Pornillos, O. W.; Morham, S. G.; Zavitz, K. H.; Wang, H. E.; Wettstein, D. A.; Stray, K. M.; Côté, M.; Rich, R. L.; Myszka, D. G.; Sundquist, W. I. Tsg101 and the vacuolar protein sorting pathway are essential for HIV-1 budding. *Cell* **2001**, *107*, 55–65.
(8) Lee, S.; Joshi, A.; Nagashima, K.; Freed, E. O.; Hurley, J. H. Structural basis for viral late-domain binding to Alix. *Nat. Struct. Mol. Biol.* **2007**, *14*, 194–199.
(9) Fisher, R. D.; Chung, H. Y.; Zhai, Q.; Robinson, H.; Sundquist, W. I.; Hill, C. P. Structural and biochemical studies of ALIX/AIP1 and its role in retrovirus budding. *Cell* **2007**, *128*, 841–52.
(10) Göttlinger, H. G. How HIV-1 hijacks ALIX. *Nat. Struct. Mol. Biol.* **2007**, *14*, 254–256.
(11) Briggs, J. A.; Simon, M. N.; Gross, I.; Kräusslich, H. G.; Fuller, S. D.; Vogt, V. M.; Johnson, M. C. The stoichiometry of Gag protein in HIV-1. *Nat. Struct. Mol. Biol.* **2004**, *11*, 672–675.
(12) Ono, A.; Freed, E. O. Binding of human immunodeficiency virus type 1 Gag to membrane: Role of the matrix amino terminus. *J. Virol.* **1999**, *73*, 4136–4144.
(13) Bouamr, F.; Scarlata, S.; Carter, C. A. Role of myristylation in HIV-1 Gag assembly. *Biochemistry* **2003**, *42*, 6408–6417.
(14) Welsch, S.; Muller, B.; Kräusslich, H. G. More than one door − Budding of enveloped viruses through cellular membranes. *FEBS Lett.* **2007**, *581*, 2089–2097.
(15) Swanstrom, R.; Wills, J. W. Synthesis, assembly, and processing of viral proteins. In *Retroviruses*; Coffin, J. M., Hughes, S. H., Varmus, H. E., Eds.; Cold Spring Harbor Laboratory: Cold Spring Harbor, NY, 1997; pp 263−334.
(16) Dussupt, V.; Javid, M. P.; Abou-Jaoudé, G.; Jadwin, J. A.; de La Cruz, J.; Nagashima, K.; Bouamr, F. The nucleocapsid region of HIV-1 Gag cooperates with the PTAP and LYPXnL late domains to recruit the cellular machinery necessary for viral budding. *PLoS Pathog.* **1995**, *5*, No. e1000339.
(17) Huang, M.; Orenstein, J. M.; Martin, M. A.; Freed, E. O. p6Gag is required for particle production from full-length human immunodeficiency virus type 1 molecular clones expressing protease. *J. Virol.* **1995**, *69*, 6810–6818.
(18) Ebbets-Reed, D.; Scarlata, S.; Carter, C. A. The major homology region of the HIV-1 gag precursor influences membrane affinity. *Biochemistry* **1996**, *35*, 14268–14275.

(19) Waheed, A. A.; Freed, E. O. Peptide inhibitors of HIV-1 egress. *ACS Chem. Biol.* **2008**, *3*, 745–747.
(20) Salgado, G. F.; Marquant, F. R.; Vogel, A.; Alves, I. D.; Feller, S. E.; Morellet, N.; Bouaziz, S. Structural studies of HIV-1 Gag p6ct and its interaction with Vpr determined by solution nuclear magnetic resonance. *Biochemistry* **2009**, *48*, 2355–2367.
(21) Ehrlich, L.; Fong, S.; Scarlata, S.; Zybarth, G.; Carter, C. Partitioning of HIV-1 Gag and Gag-related proteins to membranes. *Biochemistry* **1996**, *35*, 3933–3943.
(22) Pincetic, A.; Leis, J. The mechanism of budding of retroviruses from cell membranes. *Adv. Virol.* **2009** No. 623969.
(23) Salamon, Z; Brown, M. F.; Tollin, G. Plasmon resonance spectroscopy: Probing molecular interactions within membranes. *Trends Biochem. Sci.* **1999**, *24*, 213–219.
(24) Tollin, G.; Salamon, Z.; Hruby, V. J. Techniques: Plasmon-waveguide resonance (PWR) spectroscopy as a tool to study ligand-GPCR interactions. *Trends Pharmacol. Sci.* **2003**, *24*, 655–659.
(25) Alves, I. D.; Park, C. K.; Hruby, V. J. Plasmon resonance methods in GPCR signaling and other membrane events. *Curr. Protein Pept. Sci.* **2005**, *6*, 293–312.
(26) Salamon, Z.; Tollin, G. Graphical analysis of mass and anisotropy changes observed by plasmon-waveguide resonance spectroscopy can provide useful insights into membrane protein function. *Biophys. J.* **2004**, *86*, 2508–2516.
(27) Alves, I. D.; Salgado, G. F. J.; Salamon, Z.; Brown, M. F.; Tollin, G.; Hruby, Victor J. Phosphatidylethanolamine enhances rhodopsin photoactivation and transducin binding in a solid supported lipid bilayer as determined using plasmon-waveguide resonance spectroscopy. *Biophys. J.* **2005**, *88*, 198–210.
(28) Brooks, B. R.; Bruccoleri, R. E.; Olafson, B. D.; States, D. J.; Swaminathan, S.; Karplus, M. CHARMM: A program for macromolecular energy, minimization, and dynamics calculations. *J. Comput. Chem.* **1983**, *4*, 187–217.
(29) Klauda, J. B.; Brooks, B. R.; MacKerell, A. D.; Venable, R. M.; Pastor, R. W. An ab initio study on the torsional surface of alkanes and its effect on molecular simulations of alkanes and a DPPC bilayer. *J. Phys. Chem. B* **2005**, *109*, 5300–5531.
(30) Fossen, T.; Wray, V.; Bruns, K.; Rachmat, J.; Henklein, P.; Tessmer, U.; Maczurek, A.; Klinger, P.; Schubert, U. Solution structure of the human immunodeficiency virus type 1 p6 protein. *J. Biol. Chem.* **2005**, *280*, 42515–42527.
(31) Gumbart, J.; Wang, Y.; Aksimentiev, A.; Tajkhorshid, E.; Schulten, K. Molecular dynamics simulations of proteins in lipid bilayers. *Curr. Opin. Struct. Biol.* **2005**, *15*, 423–431.
(32) Essmann, U.; Perera, L.; Berkowitz, M. L.; Darden, T.; Lee, H.; Pedersen, L. G. A smooth particle mesh Ewald method. *J. Chem. Phys.* **1995**, *103*, 8577–8593.
(33) Facke, M.; Janetzko, A.; Shoeman, R. L.; Krausslich, H. G. A large deletion in the matrix domain of the human immunodeficiency virus gag gene redirects virus particle assembly from the plasma membrane to the endoplasmic reticulum. *J. Virol.* **1993**, *67*, 4972–4980.
(34) Pettersen, E. F.; Goddard, T. D.; Huang, C. C.; Couch, G. S.; Greenblatt, D. M.; Meng, E. C.; Ferrin, T. E. UCSF Chimera - A visualization system for exploratory research and analysis. *J. Comput. Chem.* **2004**, *25*, 1605–1612.
(35) Usami, Y.; Popov, S.; Popova, E.; Inoue, M.; Weissenhorn, W.; Gottlinger, H. G. The ESCRT pathway and HIV-1 budding. *Biochem. Soc. Trans.* **2009**, *37*, 181–184.
(36) Morellet, N.; Roques, B. P.; Bouaziz, S. Structure-function relationship of Vpr: Biological implications. *Curr. HIV Res.* **2009**, *7* (2), 1570–1162.
(37) Wenk, M. R. Lipidomics of host-pathogen interactions. *FEBS Lett.* **2006**, *580*, 5541–5551.
(38) Welker, R.; Hohenberg, H.; Tessmer, U.; Huckhagel, C.; Kräusslich, H.-G. Biochemical and structural analysis of isolated mature cores of human immunodeficiency virus type 1. *J. Virol.* **2000**, *74*, 1168–1177.
(39) Accola, M. A.; Öhagen, A.; Göttlinger, H. G. Isolation of human immunodeficiency virus type 1 cores: Retention of Vpr in the absence of p6gag. *J. Virol.* **2000**, *74*, 6198–6202.
(40) Resh, M. D. Intracellular trafficking of HIV-1 Gag: How Gag interacts with cell membranes and makes viral particles. *AIDS Rev.* **2005**, *7*, 84–91.
(41) Fleming, E.; Maharaj, N. P.; Chen, J. L.; Nelson, R. B.; Elmore, D. E. Effect of lipid composition on buforin II structure and membrane entry. *Proteins: Struct., Funct., Bioinf.* **2008**, *73*, 480–491.